YENNIE–FRAUTSCHI–SUURA FOR FUTURE LEPTON COLLIDERS*

Alan Price

Jagiellonian University, Łojasiewicza 11, 30-348 Kraków, Poland

Received 30 May 2024, accepted 5 June 2024, published online 5 August 2024

The proposed future lepton collider experiments will reach an unprecedented level of precision for electroweak pseudo-observables. To ensure the success of these experiments, the corresponding theoretical uncertainty must be at least of the same order if not lower. One dominant source of uncertainty is due to the treatment of photon radiation and the potentially large logarithms which need to be resummed. In this work, we present the Yennie–Frautschi–Suura theorem and its implementation in the Sherpa Monte-Carlo framework. In particular, we focus on the automated inclusion of next-to-leading order electroweak corrections.

DOI:10.5506/APhysPolBSupp.17.5-A8

1. Introduction

With an unprecedented amount of data gathered, the Large Hadron Collider (LHC) continues to provide a rich environment that allows us to test further and scrutinise our knowledge of fundamental particles and their interactions with matter. The discovery of the Higgs boson by the ATLAS [1] and CMS [2] collaborations provided conclusive validation of spontaneously broken gauge theories as the construction principle underpinning our understanding of Nature, with the Standard Model (SM) of particle physics as its manifest realization. To date, there has not been any direct discovery of physics beyond the SM at the LHC. Still, some observations cannot be fully explained within its framework: for example, the observation of non-zero neutrino masses, dark matter and energy, and the anti-matter–matter asymmetry.

While the LHC, and potential hadron collider successors, may yet provide a deeper understanding of the nature of the Higgs boson, a future lepton–lepton collider or "Higgs factory" could provide unprecedented

* Presented at the 30$^{\text{th}}$ Cracow Epiphany Conference on *Precision Physics at High Energy Colliders*, Cracow, Poland, 8–12 January, 2024.

measurements of the electroweak nature of the SM and thus provide an alternative experimental avenue for the community to explore [3]. Due to their beams composed of elementary particles, unlike a hadron machine, a lepton–lepton collider has a very clean initial state, which facilitates measurements of electroweak pseudo-observables (EWPO) [4] with unprecedented precision.

To take full advantage of these highly precise machines, the corresponding theory uncertainties have to be smaller or, at least, match the size of the experimental ones, see Table 1 for some examples. There are two main types of theory uncertainties that need to be addressed by the community for the successful analysis of the experimental results: parametric uncertainties, which reflect our limited knowledge of the fundamental SM input parameters, and uncertainties due to missing higher-order terms in our perturbative calculations. A large source of intrinsic theoretical uncertainties are corrections due to QED radiation, where improvements by factors of 2–100, depending on the observable, are mandatory to reduce the QED uncertainties to an acceptable level. This demand reflects the simple fact that QED effects of the order of 0.1%, which could be safely ignored at LEP, turn into limiting factors in the full analysis of experimental results at future Higgs factories.

Table 1. The current systematic and statistical uncertainties on QED sensitive observables, with terms in $\{\ldots\}$ denoting the contributions to QED alone. The FCC-ee uncertainty estimates have been taken from [5], the overall table has been reproduced from [6].

Observable	Where from	Current (LEP)	FCC (stat.)	FCC (syst.)	$\frac{\text{Now}}{\text{FCC}}$
M_Z [MeV]	Z linesh. [7]	$91187.5 \pm 2.1\{0.3\}$	0.005	0.1	3
Γ_Z [MeV]	Z linesh. [7]	$2495.2 \pm 2.1\{0.2\}$	0.008	0.1	2
$R_l^Z = \Gamma_h/\Gamma_l$	$\sigma(M_Z)$ [8]	$20.767 \pm 0.025\{0.012\}$	6×10^{-5}	1×10^{-3}	12
σ^0_{had} [nb]	σ^0_{had} [7]	$41.541 \pm 0.037\{0.025\}$	0.1×10^{-3}	4×10^{-3}	6
N_ν	$\sigma(M_Z)$ [7]	$2.984 \pm 0.008\{0.006\}$	5×10^{-6}	1×10^{-3}	6
N_ν	$Z\gamma$ [9]	$2.69 \pm 0.15\{0.06\}$	0.8×10^{-3}	$< 10^{-3}$	60
$\sin^2\theta_W^{\text{eff}}\times 10^5$	$A_{\text{FB}}^{\text{lept}}$ [8]	$23099 \pm 53\{28\}$	0.3	0.5	55
$\sin^2\theta_W^{\text{eff}}\times 10^5$	$\langle\mathcal{P}_\tau\rangle$, $A_{\text{FB}}^{\text{pol},\tau}$ [7]	$23159 \pm 41\{12\}$	0.6	< 0.6	20
M_W [MeV]	ADLO [10]	$80376 \pm 33\{6\}$	0.5	0.3	12
$A_{\text{FB},\mu}^{M_Z\pm 3.5\,\text{GeV}}$	$\frac{\mathrm{d}\sigma}{\mathrm{d}\cos\theta}$ [7]	$\pm 0.020\{0.001\}$	1.0×10^{-5}	0.3×10^{-5}	100

In Sherpa, as in many other Monte Carlo event generators [11–13], this has so far been included through the structure function approach [14] which resums the large logarithms associated to multiple (collinear) photon emission through the Dokshitser–Gribov–Lipatov–Altarelli–Parisi (DGLAP) equations [15–18]. While Sherpa implements the well-known leading-order accuracy [19–21], in recent years, the structure functions have been extended to next-to-leading logarithmic accuracy [22, 23]. However, instead of further improving the structure function approach implementation in Sherpa, we will here calculate the emission of soft photons and resum the associated logarithms in the Yennie–Frautschi–Suura formulation (YFS) [24]. In particular, we will show how to include next-to-leading order (NLO) corrections automatically in this framework. The use of YFS in Monte Carlo simulations has been pioneered by the work of Jadach and his collaborators [25–30]. The sophisticated and technical approach that they used allow the LEP experiments to push the frontier of precision measurements and will be crucial to the success of any future lepton collider.

2. Theory

In their seminal paper Yennie, Frautschi, and Suura [24] showed that, to all orders, the infrared divergences (IR) associated with the emission of real and virtual photons can be resummed to infinite order. With this method, one can rewrite the entire perturbative series into a sum of IR finite terms. This allows you to include higher-order perturbative corrections in a systematic way. In addition, the YFS approach *explicitly* generates resolved photons, with a resolution criterion given by an energy and angle cut-off. This allows us to generate the full kinematic structure of scattering events, leading to a straightforward implementation of the YFS method as both cross-section calculator and event generator.

Summing over all real and virtual photon emissions for an arbitrary $2 \to N$ scattering, the total cross section is given by

$$\begin{aligned} \mathrm{d}\sigma \;=\; & \sum_{n_\gamma=0}^{\infty} \frac{1}{n_\gamma!}\, \mathrm{d}\Phi_Q \left[\prod_{i=1}^{n_\gamma} \mathrm{d}\Phi_i^\gamma\right] (2\pi)^4\, \delta^4 \\ & \left(\sum_{i=1}^{2} p_i - \sum_{j=3}^{N+2} q_j - \sum_{k=1}^{n_\gamma} k_k\right) \left|\sum_{\bar{n}_\gamma=0}^{\infty} \mathcal{M}_{n_\gamma}^{\bar{n}_\gamma+\frac{1}{2}n_\gamma}\right|^2 , \end{aligned} \tag{1}$$

where the outgoing momenta q_j emerge from the original p_j after the effect of the real photon emissions has been taken into account. Here, $\mathrm{d}\Phi_Q$ denotes the modified final-state phase-space element, the $\mathrm{d}\Phi_i^\gamma$ are the phase-space elements spanned by the n_γ real photon momenta k_i emitted off the leading order configuration. Similarly, $\bar{n}_\gamma$ counts the number of virtual photons added to it. The indices i and j matrix elements $\mathcal{M}_i^j$ indicate the number of real photons, i, and the overall additional orders in α, j, relative to the Born configuration.

To analyse the structure of the resummation and its fixed-order improvements, consider the case of a single virtual photon. In the soft limit, the matrix element factorises as

$$\mathcal{M}_0^1 = \alpha B M_0^0 + M_0^1 \,. \tag{2}$$

Therein, α is the QED coupling constant, B is an integrated off-shell eikonal encoding the universal soft-photon limit [31], and $\mathcal{M}_0^0 = M_0^0$ is the leading order matrix element. Then, the finite remainder M_0^1 is the infrared-subtracted matrix element including one virtual photon. YFS showed that the insertion of further virtual photons leads to a power series and due to the Abelian nature of QED and the absence of collinear singularities in the soft-photon limit, this can be further generalised to a squared matrix elements that include any number of additional real photon emissions, such that

$$\left| \sum_{\bar{n}_\gamma=0}^{\infty} \mathcal{M}_{n_\gamma}^{\bar{n}_\gamma + \frac{1}{2}n_\gamma} \right|^2 = \exp(2\alpha B) \left| \sum_{\bar{n}_\gamma}^{\infty} M_{n_\gamma}^{\bar{n}_\gamma + \frac{1}{2}n_\gamma} \right|^2 \,. \tag{3}$$

By construction, $M_{n_\gamma}^{\bar{n}_\gamma + \frac{1}{2}n_\gamma}$ is completely free of soft singularities due to virtual photons but it will still contain those due to real photons. Similarly, for the real-photon emissions, the factorization occurs at the level of squared matrix elements and by extracting all real-emission soft-photon divergences through eikonal factors, the squared matrix element for any n_γ real emissions, summed over all possible virtual photon corrections, can be written as

$$\begin{aligned}
\left(\frac{1}{2(2\pi)^3}\right)^{n_\gamma} \left| \sum_{\bar{n}_\gamma=0}^{\infty} M_{n_\gamma}^{\bar{n}_\gamma + \frac{1}{2}n_\gamma} \right|^2 &= \tilde{\beta}_0 \prod_{i=1}^{n_\gamma} \left[\tilde{S}\left(k_i\right)\right] \\
+ \sum_{i=1}^{n_\gamma} \left[\frac{\tilde{\beta}_1\left(k_i\right)}{\tilde{S}\left(k_i\right)}\right] \prod_{j=1}^{n_\gamma} \left[\tilde{S}\left(k_j\right)\right] &+ \sum_{\substack{i,j=1 \\ i<j}}^{n_\gamma} \left[\frac{\tilde{\beta}_2\left(k_i, k_j\right)}{\tilde{S}\left(k_i\right)\tilde{S}\left(k_j\right)}\right] \prod_{l=1}^{n_\gamma} \left[\tilde{S}\left(k_l\right)\right] + \dots \\
+ \tilde{\beta}_{n_\gamma - 1}\left(k_1, \dots, k_{i-1}, k_{i+1}, \dots, k_{n_\gamma}\right) \sum_{i=1}^{n_\gamma} \tilde{S}\left(k_i\right) &+ \tilde{\beta}_{n_\gamma}\left(k_1, \dots, k_{n_\gamma}\right) \,,
\end{aligned} \tag{4}$$

where

$$\tilde{\beta}_{n_\gamma} = \sum_{\bar{n}_\gamma=0}^{\infty} \tilde{\beta}_{n_\gamma}^{\bar{n}_\gamma + n_\gamma} \,. \tag{5}$$

The $\tilde{\beta}_{n_\gamma}^{\bar{n}_\gamma+n_\gamma}$ are the infrared-finite squared matrix elements. They correspond to the Born level process plus emissions of n_γ real and $\bar{n}_\gamma$ virtual photons of the order of $n_\gamma + \bar{n}_\gamma$ in the QED coupling α. To recombine all terms into an expression for the inclusive cross section and facilitate the cancellation of all infrared singularities, it is useful to define an unresolved region Ω in which the kinematic impact of any real-photon emission is unimportant. Integrating over this unresolved real emission phase space gives the integrated on-shell eikonal $\tilde{B}$,

$$2\alpha\tilde{B}(\Omega) = \int \frac{\mathrm{d}^3k}{k^0}\,\tilde{S}\,(k)\,[1 - \Theta(k,\Omega)]\ , \tag{6}$$

which contains all infrared poles due to real soft photon emission. Substituting this expression back into Eq. (1), the contributions originating from $\tilde{B}$ for all n_γ photons again exponentiate. This yields

$$\begin{aligned}\mathrm{d}\sigma \;&=\; \sum_{n_\gamma=0}^{\infty} \frac{e^{Y(\Omega)}}{n_\gamma!}\,\mathrm{d}\Phi_Q \left[\prod_{i=1}^{n_\gamma} \mathrm{d}\Phi_i^\gamma\,\tilde{S}\,(k_i)\ \Theta\,(k_i,\Omega)\right] \\ &\quad\times \left(\tilde{\beta}_0 + \sum_{j=1}^{n_\gamma}\frac{\tilde{\beta}_1(k_j)}{\tilde{S}\,(k_j)} + \sum_{j,k=1^{j<k}}^{n_\gamma}\frac{\tilde{\beta}_2(k_j,k_k)}{\tilde{S}\,(k_j)\,\tilde{S}\,(k_k)} + \cdots\right)\ ,\end{aligned} \tag{7}$$

with the YFS form factor

$$Y(\Omega) = 2\alpha\left[B + \tilde{B}(\Omega)\right]\ . \tag{8}$$

Therein, all infrared singularities originating from real and virtual soft-photon emission, contained in $\tilde{B}$ and B, respectively, cancel, leaving a finite remainder.

In figure 1, we show the energy-dependent Higgs production cross section in various channels, and compare the results at the Born level with those obtained by including QED ISR using YFS. The QED ISR tends to increase the cross sections at high c.m. energies in those processes that are driven by the exchange of an s-channel propagator, such as $e^+e^- \to ZH$ and the top-associated production, while it tends to decrease the cross section at their peaks. The increase can be thought of as the effect of some form of a "radiative return" to the peak, while the decrease at the peak can be understood as a "washing out" of the large peak cross section by reducing the c.m. energy due to the ISR. Conversely, QED ISR decreases the production cross sections throughout in those processes that are t-channel-dominated. With these results, we can also see how our implementation of the YFS algorithm is process-independent [31].

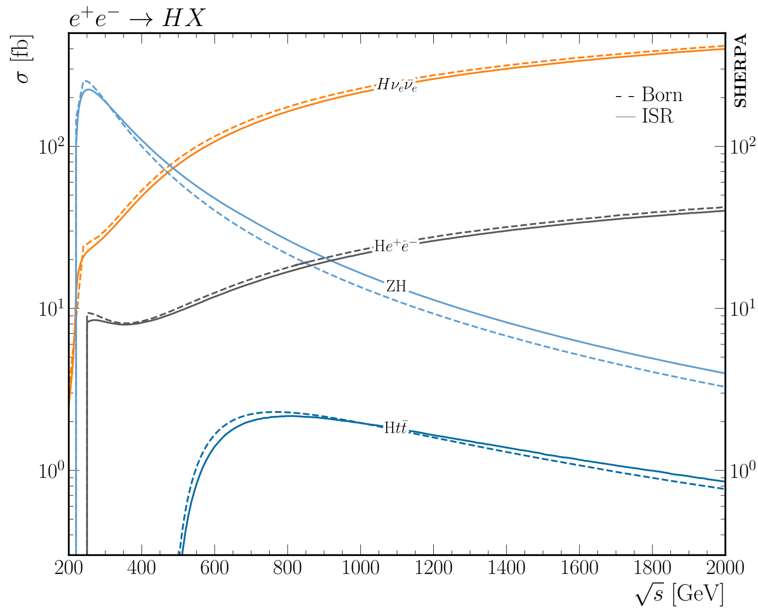

Fig. 1. Total cross section for the HX production. Dashed lines represent the Born-level cross section, while the solid includes YFS resummation.

2.1. Virtual corrections

We can now exploit the IR finiteness of individual $\tilde{\beta}$ terms to incorporate the one-loop electroweak corrections for various e^+e^- processes and consistently match them with the YFS resummation. The one-loop IR finite residue is given by

$$\tilde{\beta}_0^1\left(\Phi_n\right) = \mathcal{V}\left(\Phi_n\right) - \sum_{ij} \mathcal{D}_{ij}\left(\Phi_{ij}\right) . \tag{9}$$

In equation (9), the first term represents the full one-loop correction, which may contain IR divergences that can be regulated using a fictitious photon mass or dimensional regularization. The second term corresponds to the YFS subtraction for virtual divergences, where we sum over the relevant dipoles contributing to the calculation. This term is computed using massive regularization, requiring the inclusion of a fictitious photon mass. Alternatively, dimensional regularization can be used for this subtraction. However, since we are dealing with IR divergences arising solely from QED, the introduction of massive regularization poses no issues. In figure 2, we show how the YFS subtraction behaves for the virtual amplitudes. We consider the $e^+e^- \to \mu^+\mu^-$ process and calculate the full IR divergent one-loop corrections to this process with Recola for various fictitious photon masses. In Sherpa, we then calculate the subtraction term, consisting of six dipole terms times the Born, and subtract the two quantities from each other. We see that the IR divergences, which appear as logarithms of the photon mass, cancel exactly between the two terms leading to an IR finite results.

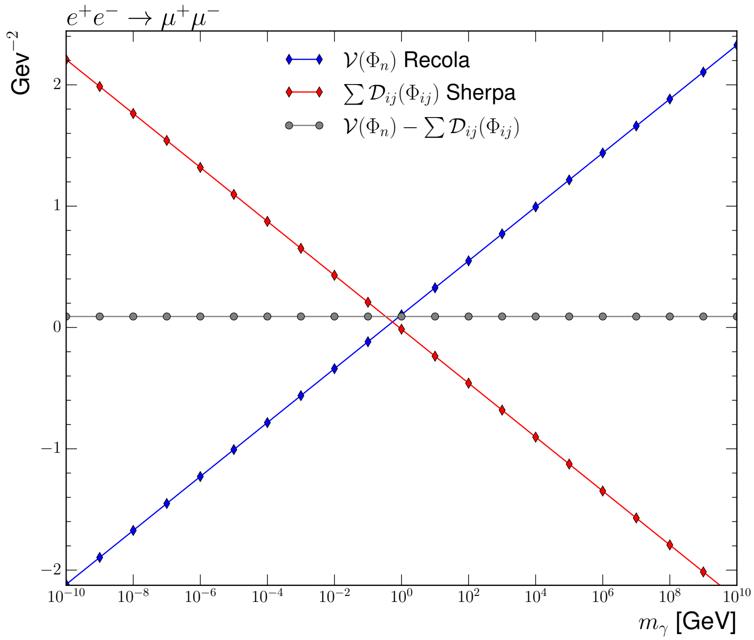

Fig. 2. Cancellation of the virtual IR divergences using YFS subtraction.

2.2. Real corrections

The one real photon correction to the Born process can be rendered IR finite within the YFS framework as follows:

$$\tilde{\beta}_1^1\left(\mathit{\Phi}_{n+1}\right) = \frac{1}{2(2\pi)^3}\left|\mathcal{M}_0^{\frac{1}{2}}\right|^2 - \tilde{S}\left(k\right)\tilde{\beta}_0^0\left(\mathit{\Phi}_n\right)\,, \tag{10}$$

where $\mathcal{M}_0^{\frac{1}{2}}$ is the $\mathcal{O}(\alpha)$ real correction and since it is purely a tree-level amplitude, it can also be calculated automatically using modern amplitude methods. There exist many automated tools [12, 32–35] capable of calculating these amplitudes. For this study, we use Sherpa's internal matrix-element generators (MEGs), namely AMEGIC [32] and COMIX [33]. Both MEGs can calculate the squared amplitudes for complicated final states as chains of subsequent decays in the narrow-width approximation, taking all effects due to spin and color correlations into account. They have already been used in the automated calculation of the $\tilde{\beta}_0^0$ terms [31]. In figure 3, we show the behaviour of equation (10) as we take the soft limit. For this comparison, we take a random phase-space point with one sufficiently hard photon and calculate its contribution to the real correction. We then artificially lower the energy of this photon, remap the phase-space point to compensate for this, and reevaluate equation (10). We continue to do this until the photon reaches the IR cutoff, below which the subtraction becomes unstable. This instability is not physical and if one so desires it can be pushed to lower values simply by changing the cutoff value. Figure 3 shows that as the photon becomes softer and softer, the real correction converges to the subtraction term as expected.

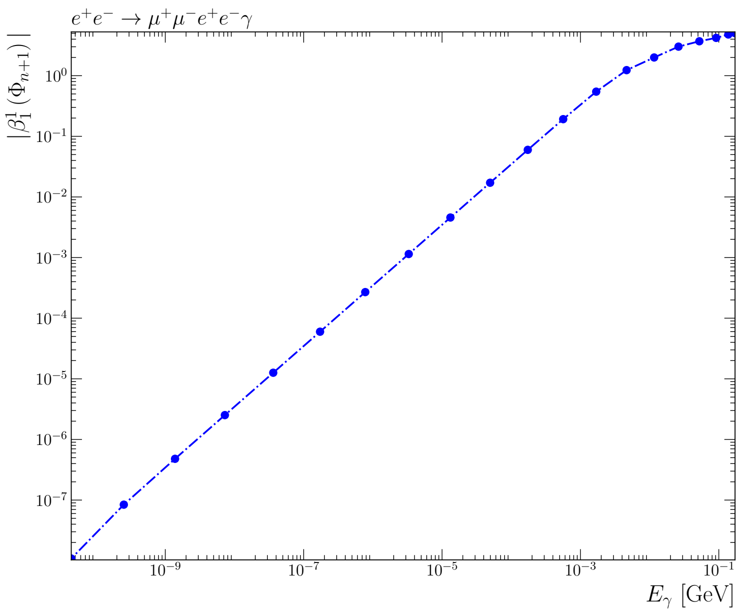

Fig. 3. IR finiteness of the real corrections as the photon approaches the soft limit.

3. Conclusion

Given the expected precision at the proposed Higgs factories, the need to improve the accuracy of Monte Carlo tools is a high priority for the theory community. The large QED errors will require dramatic improvements to ensure we can match the experimental precision. The resummation of potentially large logarithms will be mandatory to reach the theoretical precision needed at Higgs factories. In addition to the resummation, matching to higher-order perturbative corrections will also be required. We have shown that the YFS algorithm can be implemented in an automated process-independent manner. This not only allows us to resum, to all orders, of soft logarithms but also explicitly generates resolved photons. With this sophisticated phase-space treatment, we are able to automate NLO real corrections with a subtraction scheme that is highly stable in the soft limit. Additionally, we have shown that the inclusion of virtual corrections can be achieved using automated one-loop providers with an automated subtraction scheme implemented in Sherpa. It is envisioned that this approach will be extended to NNLO, however the limitations for this will be the availability of two-loop electroweak corrections.

This work is funded by grant No. 2023/50/A/ST2/00224 of the National Science Centre (NCN), Poland and also by the Priority Research Area Digiworld under the program Excellence Initiative — Research University at the Jagiellonian University in Cracow.

REFERENCES

[1] ATLAS Collaboration (G. Aad *et al.*), *Phys. Lett. B* **716**, 1 (2012).

[2] CMS Collaboration (S. Chatrchyan *et al.*), *Phys. Lett. B* **716**, 30 (2012).

[3] J. de Blas *et al.*, *J. High Energy Phys.* **2020**, 139 (2020).

[4] A. Freitas *et al.*, `arXiv:1906.05379 [hep-ph]`.

[5] FCC Collaboration (A. Abada *et al.*), *Eur. Phys. J. C* **79**, 474 (2019).

[6] S. Jadach, M. Skrzypek, *Eur. Phys. J. C* **79**, 756 (2019).

[7] ALEPH, DELPHI, L3, OPAL, SLD collaborations, LEP Electroweak Working Group, SLD Electroweak and Heavy Flavour Groups (S. Schael *et al.*), *Phys. Rep.* **427**, 257 (2006).

[8] ALEPH, DELPHI, L3, OPAL collaborations, LEP Electroweak Working Group, SLD Heavy Flavour and Electroweak Groups (D. Abbaneo *et al.*), `arXiv:hep-ex/0112021`.

[9] OPAL Collaboration (G. Abbiendi *et al.*), *Eur. Phys. J. C* **18**, 253 (2000).

[10] ALEPH, DELPHI, L3, OPAL collaborations, LEP Electroweak Working Group (S. Schael *et al.*), *Phys. Rep.* **532**, 119 (2013).

[11] M. Bahr *et al.*, *Eur. Phys. J. C* **58**, 639 (2008).

[12] J. Alwall *et al.*, *J. High Energy Phys.* **2011**, 128 (2011).

[13] T. Sjöstrand, S. Mrenna, P.Z. Skands, *J. High Energy Phys.* **2006**, 026 (2006).

[14] E.A. Kuraev, V.S. Fadin, *Sov. J. Nucl. Phys.* **41**, 466 (1985).

[15] G. Altarelli, G. Parisi, *Nucl. Phys. B* **126**, 298 (1977).

[16] V.N. Gribov, L.N. Lipatov, *Sov. J. Nucl. Phys.* **15**, 438 (1972).

[17] L.N. Lipatov, *Yad. Fiz.* **20**, 181 (1974).

[18] Y.L. Dokshitzer, *Sov. Phys. JETP* **46**, 641 (1977).

[19] M. Cacciari, A. Deandrea, G. Montagna, O. Nicrosini, *Eur. Phys. Lett.* **17**, 123 (1992).

[20] M. Skrzypek, *Acta Phys. Pol. B* **23**, 135 (1992).

[21] M. Skrzypek, S. Jadach, *Z. Phys. C* **49**, 577 (1991).

[22] V. Bertone, M. Cacciari, S. Frixione, G. Stagnitto, *J. High Energy Phys.* **2020**, 135 (2020); *Erratum ibid.* **2022**, 108 (2022).

[23] S. Frixione, *J. High Energy Phys.* **2019**, 158 (2019).

[24] D.R. Yennie, S.C. Frautschi, H. Suura, *Ann. Phys.* **13**, 379 (1961).

[25] S. Jadach, W. Płaczek, B.F.L. Ward, *Phys. Lett. B* **390**, 298 (1997).

[26] S. Jadach *et al.*, *Comput. Phys. Commun.* **119**, 272 (1999).

[27] S. Jadach *et al.*, *Comput. Phys. Commun.* **140**, 432 (2001).

[28] B.F.L. Ward, S. Jadach, Z. Was, *Nucl. Phys. B Proc. Suppl.* **116**, 73 (2003).

[29] S. Jadach, B.F.L. Ward, Z. Wąs, *Comput. Phys. Commun.* **130**, 260 (2000).

[30] S. Jadach, B.F.L. Ward, Z. Wąs, *Phys. Rev. D* **63**, 113009 (2001).

[31] F. Krauss, A. Price, M. Schönherr, *SciPost Phys.* **13**, 026 (2022).

[32] F. Krauss, R. Kuhn, G. Soff, *J. High Energy Phys.* **2002**, 044 (2002).

[33] T. Gleisberg, S. Höche, *J. High Energy Phys.* **2008**, 039 (2008).

[34] M.L. Mangano *et al.*, *J. High Energy Phys.* **2003**, 001 (2003).

[35] W. Kilian, T. Ohl, J. Reuter, *Eur. Phys. J. C* **71**, 1742 (2011).